Volume 255, number 1, 47–52 FEBS 07559 September 1989

Direct identification of the fluoroaluminate and fluoroberyllate species responsible for inhibition of the mitochondrial F_1-ATPase

Alain Dupuis, Jean-Paul Issartel and Pierre V. Vignais

Laboratoire de Biochimie, LBIO DRF, Centre d'Etudes Nucléaires de Grenoble, 85X, 38041 Grenoble Cedex, France

Received 28 June 1989

In the presence of ADP, fluoroaluminate and fluoroberyllate inhibit irreversibly the soluble mitochondrial F_1-ATPase. We report here direct evidence that this inhibition is related to the tight binding of [^{3}H]ADP, beryllium and fluoride to the enzyme. In the case of beryllium-induced inhibition, the stoichiometry of bound species is 1 mol [^{3}H]ADP, 1 mol beryllium and 2 or 3 mol fluoride depending on the initial fluoride concentration used, which indicates that both the combinations ADP_1,Be_1,F_2 and ADP_1,Be_1,F_3 are competent for inhibition. In the case of aluminium-induced inhibition, the binding stoichiometry of 4 mol fluoride per mol [^{3}H]ADP favours the following combination of bound species ADP_1,Al_1,F_4. These results favour a model where fluorometals mimic phosphate and form an abortive complex with ADP in the catalytic site(s) of F_1.

Fluoride; Beryllium; Aluminum; ATPase, F_1-; Nucleotide analogue

1. INTRODUCTION

A number of NTP-dependent enzymes are inhibited by fluoride, while G-proteins are activated [1,2]. A breakthrough in the understanding of the mechanism of action of fluoride was the finding, by Sternweis and Gilman [3], that the fluoride-dependent activation of adenylate cyclase requires aluminium or beryllium ions. Later, Bigay et al. [4,5] proposed that the fluorometal complex AlF_4^-, as well as BeF_3^-, might act as a phosphate analogue, and that AlF_4^- of BeF_3, in the form of tetrahedral complexes structurally similar to phosphate, combines with GDP in the nucleotide-binding site of transducin. The postulated GDP-AlF_3 complex mimicks GTP, and promotes activation of transducin, as does GTP. Such a model predicts that enzymes with a binding site for NTP would recognize NDP-AlF_3 complexes as NTP analogues. Indeed, it was recently shown that phospholipase C-coupled G-protein [6], hexokinase [7], tubulin [8], Na^+,K^+-ATPase [9], other P-type ATPases [10] and F_1-ATPases [11] are all sensitive to fluoride-aluminium cocktails. In the case of the mitochondrial F_1-ATPase, virtually irreversible inhibition was found to occur in the presence of aluminium, fluoride and ADP, and it was proposed that ADP-AlF_3 acts as a nonhydrolysable analogue of ATP tightly bound to a catalytic site [11].

Although the model of NDP-AlF_3 or NDP-BeF_3– complexes mimicking NTP ligands is attractive, it suffers from some drawbacks. For example, the postulate that AlF_4^- or BeF_3^- is the inhibiting species is generally based on the assumption that they are predominant in the millimolar range of fluoride concentration relevant to the biological effect. In the absence of direct evidence for this, controversies on the validity of the NDP-AlF_3 or NDP-BeF_3^- model have arisen [12–15].

We have taken advantage of the virtually irreversible nature of the inhibition of F_1-ATPase by fluoroaluminate or fluoroberyllate to determine

Correspondence address: A. Dupuis, Laboratoire de Biochimie, LBIO DRF, Centre d'Etudes Nucléaires de Grenoble, 85X, 38041 Grenoble Cedex, France

Abbreviations: NDP nucleoside diphosphate; NTP nucleoside triph.; p*F*, colog of the free fluoride concentration; CDTA *trans*-1,2 diaminocyclohexane-*N,N,N',N'*-tetraacetic acid

Published by Elsevier Science Publishers B.V. (Biomedical Division)
00145793/89/$3.50

directly the ratio of ADP, beryllium/aluminium and fluoride entrapped in F_1 as a function of the observed inhibition. These studies are reported in the present paper.

2. MATERIALS AND METHODS

Beef heart mitochondrial F_1 purification and desalting, as well as spectrophotometric measurement of the ATPase activity, were conducted as described [11]. Radioactivity was measured by scintillation counting with Ready Value Cocktail (Beckman). Protein was estimated using the Coomassie blue method [16]. Aluminium fluoride and beryllium fluoride species distributions were computerized with a TOT simulation program [17] using equilibrium constants compiled in [12].

Bound ligands (metals, fluoride and nucleotide) were measured after release from carefully desalted F_1 (see section 3) by two different methods: (i) beryllium was quantitatively released by precipitation of the enzyme with perchloric acid (final concentration 6%, w/v); the supernatant was neutralized by KOH and potassium perchlorate was removed by centrifugation; (ii) fluoride extraction by thermal denaturation [18] was preferred to acid precipitation to avoid any release of volatile HF. Both procedures proved to be quantitative, as no beryllium or fluoride was recovered by a second extraction. Furthermore, full recovery was found with internal controls containing known amounts of fluoride and beryllium. [^{3}H]ADP radioactivity was measured on the same extract obtained by termal denaturation as that used for fluoride determination. Beryllium was measured as in [19] using a standard solution of beryllium nitrate (Merck) as reference. This assay was not influenced by a number of components, including ADP, ATP, Mg^{2+}, etc. used at the same concentrations as in the presence of F_1. In the case of aluminium measurements, all techniques tested proved to be inadequate due to excessively high sensitivity to nucleotides and phosphate. Fluoride determinations were conducted with a combined fluoride electrode (Orion model 96-09) connected to an Orion Research 901 microprocessor ionialyzer with fluoride standards as references (Orion, Boston, Ma). Masking buffer (pH = 6.5) was added to the samples to yield final concentrations of 125 mM NH_4NO_3, 136 mM Na citrate and 6 mM CDTA [20]. For beryllium and fluoride assays, parallel measurements with and without an internal standard were run for each sample. Good agreements (within < 5%) was found between external and internal standards.

Chemicals were of reagent grade from various sources [11]. [^{3}H]ADP was purchased from Amersham. Ultrapure water was produced by a MilliQ apparatus (Millipore). All experiments were conducted in plastic vessels.

3. RESULTS

The inhibitory effects of aluminium or beryllium on F_1-ATPase activity are critically dependent on fluoride concentration. It was previously reported that the bell-shaped dose-effect curve for aluminium inhibition of F_1-ATPase could be fitted with the distribution curve for the AlF_4^- species present in solution [11]. However, the distribution of fluorinated species in solution at a pH of 7.5 has been recently reassessed [12] to take into account the presence of mixed fluoride and hydroxide complexes of aluminium, which were not previously considered. We have therefore used these data and have recalculated the corresponding fluorometal species distribution curves at pH 8, at which our experiments were performed. The inhibition curve of F_1-ATPase did not fit exactly with any of the predicted individual fluoroaluminium species, a possible explanation being the contribution of $AlF_3(OH)^-$ or $AlF_2(OH)_2^-$ species to an inhibitory complex (fig.1A,B). On the other hand, the experiment carried out with beryllium (fig.1C,D suggested a contribution of BeF_2, $BeF_2(OH)^-$ or BeF_3^- to the inhibitory state of F_1. These considerations show that the nature of the inhibitory

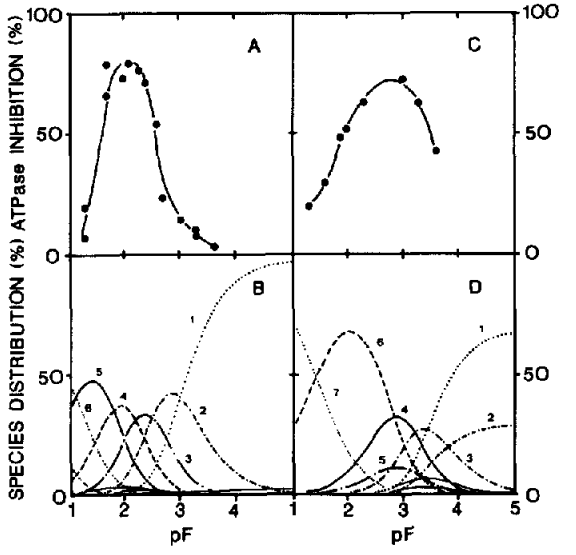

Fig.1: Effect of fluoride concentration on the development of F_1-ATPase inhibition induced by beryllium fluoridy or aluminium fluoride species. (A–C) Desalted F_1 was incubated in STNG buffer containing 2 mM $MgCl_2$, 100 μM ADP, 100 μM $AlCl_3$ (A) or 20 μM $BeCl_2$ (B) and increasing concentrations of fluoride. After 30 min at 30°C, fractions were withdrawn and assayed for ATPase activity. (B–D) Distribution of fluorometal complexes as a function of fluoride concentration. (B) fluoroaluminium species. Only the major species are identified as follows: (1): $Al(OH)_4^-$; (2): $AlF(OH)_3^-$; (3): $AlF_2(OH)_2^-$; (4): $AlF_3(OH)^-$; (5): AlF_4^-; (6): AlF_5^{2-}. (D) Fluoroberyllium species: (1) $Be(OH)^+$; (2): $Be(OH)_2$; (3): $BeF(OH)$; (4): BeF_2; (5) $BeF_2(OH)^-$; (6): BeF_3^-; (7): BeF_4^{2-}. Computerized curves at pH 8 were obtained as described in the text.

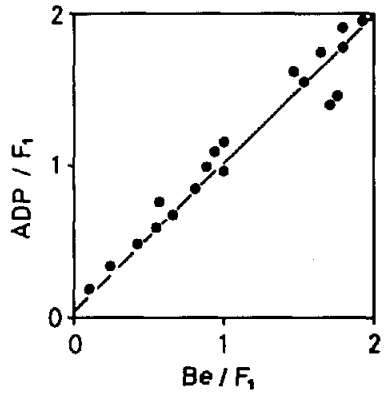

Fig.2: Determination of the amount of tightly bound beryllium and [^{3}H]ADP in relation with the inhibition of the F_1-ATPase induced by fluoroberyllate The F_1-ATPase (8 μM) was preincubated for 15 min in STNG buffer supplemented with 2 mM $MgCl_2$, 2 mM NaF and 100 μM [^{3}H]ADP at 25°C. Inhibition was then initiated by the addition of 35 μM $BeCl_2$. After varying periods of incubation, fractions were withdrawn and the partially inhibited F_1 was freed on unbound or loosely bound ligands as described in section 3. After this treatment, samples were used for measurements of enzyme activity, protein concentration, bound beryllium and bound [^{3}H]ADP (cf. section 2).

fluorometal species involved in the binding to the nucleotide site of F_1 cannot be deduced from the simple superimposition of the inhibition curves on the theoretical distribution of chemical compounds in solution. They clearly illustrate the necessity of direct measurement of bound ligands.

Inhibition of F_1 by fluoroberyllate or fluoroaluminate was nearly irreversible, which led to the conclusion that fluoroberyllate and fluoroaluminate complexes are tightly bound to F_1 [11]. Drastic depletion treatment could therefore be applied to F_1 to remove loosely bound ligands (nucleotides, fluoride and metals). On this basis, the following procedure was devised: after incubation with appropriate concentrations of [^{3}H]ADP, fluoride and metals (cf fig.2 and table 1): F_1 was freed of unbound ligands by filtration-centrifugation through a Sephadex G-50 column equilibrated in buffer composed of 0.15 M sucrose, 30 mM NaCl, 10% glycerol (w/v), 50 mM Tris-H_2SO_4, pH 8 (STNG buffer). It was then submitted to a cold chase with 0.75 mM ATP for 15 min followed by ammonium sulphate precipitation. After 30 min at 4°C, the pellet was collected by centrifugation, redissolved in 10 mM Tris-H_2SO_4pH 8 and filtered through a Sephadex G-50 centrifugation column equilibrated with the same buffer. The eluted material was then used for determination of ATPase activity, protein, beryllium and fluoride concentrations and measurement of bound radioactivity. The background was negligible, even for fluoride concentrations as high as 20 mM. The amount of tightly

Table 1

Determination of the ratio of fluoride to [^{3}H]ADP bound to F_1

Metal	p*F*	Majority species in medium[a]	Ratio of bound fluoride to bound ADP (mol/mol)[b]	Composition of bound species
Be	1.7	BeF_3^-	2.8 ± 0.2 (7)	ADP_1,Be_1,F_3
	3.0	BeF_2 + $BeF_2(OH)^-$	1.8 ± 0.1 (5)	ADP_1,Be_1,F_2
Al	1.7	$AlF_3(OH)^-$	4.0 × 0.1 (4)	ADP_1,Al_1,F_4
	2.3	$AlF_2(OH)_2^-$	4.1 × 0.1 (4)	ADP_1,Al_1,F_4

[a] Major fluoromethal species present in the solution deduced from fig.1B and D

[b] Number of independent measurements in parentheses

Experiments were conducted essentially as described in fig.2. The concentrations of beryllium and chlorides were 35 and 100 μM, respectively, and the free fluoride was as reported in the table (p*F*). At the end of the experiment, aliquots were withdrawn for determination of protein concentration. ATPase activity, bound fluoride and bound [^{3}H]ADP (see section 2).

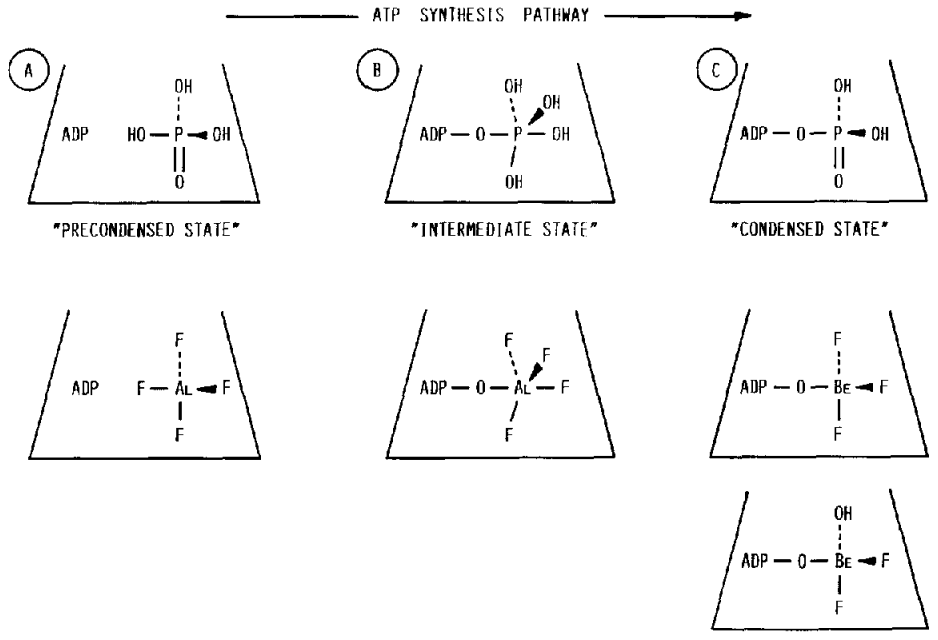

Fig.3: Schematic representation of the nucleotide complexes bound of the F_1. Nucleotide, phosphate and fluorometals are drawn bound in a schematic catalytic site. The first row symbolizes the different stages of the F_1 catalytic pathway and the second row, the corresponding inhibitory complexes.

bound beryllium and [^{3}H]ADP was first determined. As expected from the postulated model, ATPase inhibition develops concomitantly with the very tight binding of beryllium and [^{3}H]ADP to the enzyme. The data in fig.2 indicate a stoichiometric ratio of bound beryllium to bound [^{3}H]ADP of 1. This relationship holds at concentrations of free fluoride ranging between 1 mM (pF = 3) and 20 mM (pF = 1.7). A similar stoichiometry most probably holds for tightly bound aluminium and ADP. Based on this assumption, the amounts of bound fluoride per inhibitory complex were calculated, taking bound [^{3}H]ADP as reference.

The fluoride contents in the aluminium and beryllium inhibitory species are listed in table 1. The determinations of F_1 bound fluoride were carried out at two different fluoride concentrations for each metal. This procedure was adopted to check the possibility of the enzyme binding to different fluorometal species potentially involved in the inhibitory process, as suggested by the curves in fig.1. The fluoride concentrations were chosen to give F_1 inhibition values close to the maximum on either side of the inhibition peak.

In the case of beryllium, experiments were performed at free fluoride concentrations of 1 mM (pF = 3) and 20 mM (pF = 1.7). In solution, these pF values favour the formation of the BeF_2 (or BeF_2OH^-) and BeF_3^- species, respectively (cf. fig.1D). The ratios of bound fluoride per bound ADP observed under these conditions were 1.8 F^-/ADP at pF 3.0, and 2.8 F^-/ADP at pF 1.7 (table 1). These results were independent of the extent of inhibition, as similar values were obtained when F_1ATPase was inhibited at levels of either 55 or 90 %. From this, it can be concluded that, depending on the fluoride concentration, either $ADP_1Be_1F_2$ or $ADP_1Be_1F_3$ complexes may be bound at the nucleotide-binding site of F_1.

In the case of aluminium, experiments were performed at free fluoride concentrations of 5 mM (pF = 2.3) and 20 mM (pF = 1.7). In solution, these pF values favour the formation of the $AlF_2(OH)_2^-$ and $AlF_3(OH)^-$ species, respectively (cf. fig.1B). A similar ratio of 4 mol fluoride bound per mol or tightly bound ADP was found at the two different fluoride concentrations (table 1), indicating that the bound inhibiting species has a stoichiometry of association of the type $ADP_1Al_1F_4$.

4. DISCUSSION

It has been proposed previously that the biological effects of fluoride on NTP-dependent proteins in the presence of aluminium or beryllium reflect the binding of tetrahedral fluorometal complexes mimicking P_i at the level of the nucleotide-binding site [4,5]. The data of fig.1 show that the nature of the inhibitory complexes cannot readily be identified by comparing inhibition curves with the predicted fluorinated species in solution. The only conclusion that can be drawn from the bell-shaped inhibition curves shown in fig.1 is that the inhibition process is indeed mediated by the binding of a fluorometal complex to the enzyme. Thus, if fluoride and the metal were bound to different sites, as proposed in [15], then the fluoride site would have become saturated with increasing concentrations of fluoride. Thus, the inhibition curves for aluminium and for beryllium in fig.1 would have reached a plateau and this plateau would most probably have been attained at the same p*F* value for both metals.

Direct determination of bound fluoride and metals was clearly needed to define the structure of the actual inhibitory species bound to F_1. The tight binding of ADP and beryllium to F_1 in equistoichiometric amounts (fig.2) suggest that the two ligands are entrapped in the same site, resulting in the inhibition of F_1. Irrespective of the metal used, the inhibited F_1 retained fluoride (table 1). Our results provide the first demonstration of simultaneous binding of beryllium (or aluminium), fluoride and ADP to F_1. This result confirms the hypothesis of the formation of an abortive complex composed of ADP and fluorometal in the catalytic site of F_1.

Let us now discuss the structure of the ADP-fluorometal complexes deduced from our results and the similarities they share with the structure of ADP and P_i bound in the catalytic site of F_1 at three different steps of the catalytic pathway for ATP synthesis (fig.3). In the case of the inhibition of F_1-ATPase by aluminium, the amount of bound fluoride indicates the presence of AlF_4^- together with ADP in the nucleotide-binding site of the enzyme. It does not favour the existence of a bound ADP-AlF_3 complex mimicking ATP, which was postulated in a preceding model [11]. A more likely hypothesis is that AlF_4^- behaves as a high-affinity phosphate analogue but does not condense with ADP at the catalytic site of F_1. Along this line, the inhibited F_1 would be blocked in a 'precondensed state' of catalysis, analogous to (ADP + phosphate) entrapped in a closed catalytic site as illustrated in fig.3A. On the other hand, based on the necissity for phosphate to pass transiently through a pentacoordinated state in the intermediate step of the condensation of ADP and P_i in F_i, and the ability of aluminium to adopt a pentacoordinated geometry, one may hypothesize that the ADP-AlF_4^- complex mimicks the pentacoordinated 'intermediate state' in the catalytic sites of F_1 (fig.3B).

The stoichiometries of bound fluoride and bound beryllium are in agreement with the fact that BeF_2 or $BeF_2(OH)^-$, and BeF_3^-, would show similar efficiencies for F_1 inhibition. They are also consistent with the possibility that BeF_x forms complexes of the type ADP-BeF_2 or ADP-BeF_3^-, thus mimicking the condensed state in the pathway of ATP synthesis (fig.3C). In other words, fluorometals would block the F_1 in different catalytic states of the enzyme. Complementary experiments are in progress to test these hypotheses.

Acknowledgements: We thank Dr J. Willison for careful reading of this manuscript and Dr J.L. Girardet and Y. Dupont for helpful discussions.

REFERENCES

[1] Hewitt, E.J. and Nicholas, D.J.D. (1963) in: Metabolic inhibitors, vol. II (Hochster, R.M. and Quastel J.H. eds) pp 311–436. Academic Press, New York.
[2] Howlett, A.C., Sternweis, P.C., Macik, B.A., Van Arsdale, P.M. and Gilman, A.G. (1979) J. Biol. Chem. 254, 2287–2295.
[3] Sternweis, P.C. and Gilman, A.G. (1982) Proc. Natl. Acad. Sci. USA 79, 4888–4891.
[4] Bigay, J., Deterre, P., Pfister, C. and Chabre, M. (1985) FEBS Lett. 191, 181–185.
[5] Bigay, J., Deterre, P., Pfister, C. and Chabre, M. (1987) EMBO J. 6, 2907–2913.
[6] Paris, S. and Pouysségur J. (1987) J. Biol. Chem. 262, 1970–1976.
[7] Lange, A.J. Arion, W.J., Burchell, A. and Burchell, B. (1986) J. Biol. Chem. 261, 101–107.
[8] Carlier, M.F., Didry, D., Melki, R., Chabre, M. and Pantaloni, D. (1988) Biochemistry, 27, 3555–3559.
[9] Robinson, J.D., Davis, R.L. and Steinberg, M. (1986) J. Bioenerg. Biomembranes 18, 521–531.
[10] Missiaen, L., Wuytack, F., De Smedt, H., Vrolix, M. and Casteels, R. (1988) Biochem. J. 253, 827–833.

[11] Lunardi, J., Dupuis, A., Garin, J., Issartel, J.-P., Michel, L., Chabre, M. and Vignais, P.V. (1988) Proc. Natl. Acad. Sci. USA 85, 8958–8962.
[12] Martin, R.B. (1988) Biochem. Biophys. Res. Commun. 155, 1194–1200.
[13] Jackson, G.E. (1988) Inorg. Chim. Acta 151, 273–276.
[14] MacDonald, T.L. and Martin, R.B. (1988) Trends Biochem. Sci. 13, 15–19.
[15] Stadel, J.M. and Crook, S.T. (1988) Biochem J. 254, 15–20.
[16] Bradford, M.M. (1976) Anal. Biochem. 72, 248–254.
[17] Rosset, R., Desbarres, J., Jardy, A. and Bauer, D. (1985) J. Chim. Phys. 82, 647–651.
[18] Issartel, J.-P., Lunardi, J. and Vignais, P.V. (1986) J. Biol. Chem. 261, 895–901.
[19] Petidier, A., Rubio, S., Gomez-Henz, A. and Valcarcel, M. (1985) Talanta 32, 1041–1045.
[20] Vesely, J., Weiss, D. and Stulik, K. (1978) in: Analysis with ion-selective electrodes, Ellis Horwood series in analytical chemistry (Chalmers, R.D. and Masson, M. eds) pp 125–138, Wiley, New York.